Macedonian Journal of Chemistry and Chemical Engineering, Vol. **36**, No. 2, pp. 265–278 (2017)

MJCCA9 – 741 ISSN 1857-5552
e-ISSN 1857-5625
Received: September 20, 2017 DOI: 10.20450/mjcce.2017.1295
Accepted: November 22, 2017 *Original scientific paper*

CRYSTAL STRUCTURE, SPECTRAL CHARACTERIZATION, MOLECULAR MODELING STUDIES AND STRUCTURAL EFFECTS OF THE PROTON TRANSFER PROCESS FOR (*E*)-5-METHOXY-2-[(3,4-DIMETHYLPHENYLIMINO) METHYL]PHENOL

Basak Kosar Kırca[1], Gonca Özdemir Tarı[2]*, Çiğdem Albayrak Kaştaş[3], Mustafa Odabaşoğlu[4], Orhan Büyükgüngör[5]

[1]*Department of Science Education, Sinop University, Sinop, Turkey*
[2]*Vezirköprü Vocational School, Ondokuz Mayıs University, Samsun, Turkey*
[3]*Department of Chemistry, Sinop University, Sinop, Turkey*
[4]*Chemical Technology Program, Pamukkale University, Denizli, Turkey*
[5]*Department of Physics, Ondokuz Mayis University, Samsun, Turkey*
gozdemir@omu.edu.tr

The main purpose of this study is to characterize a new organic material, (*E*)-5-methoxy-2-[(3,4-dimethylphenylimino)methyl]phenol, which was synthesized and grown as a single crystal. The molecular structure and spectroscopic properties of the *ortho*-hydroxy Schiff base compound were determined by X-ray diffraction analysis, Fourier-transform infrared (FT-IR), ultraviolet-visible (UV-Vis) and nuclear magnetic resonance (NMR) spectroscopy techniques, experimentally and computationally with density functional theory (DFT) calculations. X-ray and UV-Vis studies show that the compound exists in an OH tautomeric form in the solid and solvent media. The gas phase geometry optimizations of two possible forms of the title compound, resulting from the prototropic tautomerism, were obtained using DFT calculations at the B3LYP/6-311G+(d,p) level of theory. A relaxed potential energy surface (PES) scan was performed based on the optimized geometry of the OH tautomeric form by varying the redundant internal coordinate, the O-H bond distance. According to the PES scan process, the molecular geometry is strongly affected by the intramolecular proton transfer. The calculated first hyperpolarizability indicates that the compound could be a good material for non-linear optical applications.

Keywords: Schiff base; prototropic tautomerism; intramolecular proton transfer; NLO; DFT

КРИСТАЛНА СТРУКТУРА, СПЕКТРАЛНА КАРАКТЕРИЗАЦИЈА, СТУДИИ ЗА МОЛЕКУСКО МОДЕЛИРАЊЕ И СТРУКТУРНИ ЕФЕКТИ ОД ПРОЦЕСОТ НА ПРОТОН ТРАНСФЕР ЗА (*E*)-5-МЕТОКСИ-2-[(3,4-ДИМЕТИЛФЕНИЛИМИНО)МЕТИЛ]ФЕНОЛ

Главна цел на ова истражување е да се карактеризира нов органски материјал, (*E*)-5-метокси-2-[(3,4-диметилфенилимино)метил]фенол, што беше синтетизиран и израснат како монокристал. Молекулската структура и спекторскопските својства на *орто*-хидрокси Шифовата база беа определени експериментално со помош на рендгенска дифракциска анализа, Фуриеова трансформна инфрацрвена спектроскопија (FTIR), ултравиолетова спектроскопија (UV-Vis) и нуклеарно-магнетна спектроскопска анализа и пресметковно со помош на теоријата на густината на функционалот (DFT). Испитувањата со рендгенската дифракција и UV-Vis покажуваат дека соединението постои во ОН тавтомерна форма во цврста состојба и во раствор. Геометриската оптимизација во гасна фаза на двете можни форми на наведеното соединение кои се резултат на прототропен тавтомеризам беа добиени со пресметки според DFT на нивото на теоријата B3LYP/6-311G+(d,p). Скенирањето на површината на релаксираната потенцијална енергија (PES) беше изведено врз оптимизираната геометрија на ОН тавтомерната форма со менување на редундантната внатрешна координата, должината на О–Н врската. Според скенот на процесот на PES, молекулската геометрија е под силно влијание на интрамолекулскиот

трансфер на протони. Пресметаната прва хиперполаризабилност укажува дека соединението би било добар материјал за нелинеарни оптички апликации.

Клучни зборови: Шифови бази; прототропна тавтомерија; меѓумолекулски трансфер на протони; NLO; DFT

1. INTRODUCTION

The reaction of an aldehyde and a primary amine forms a Schiff base compound with a C=N double bond. Schiff bases have a wide range of applications in the fields of coordination chemistry, biochemistry, pharmacy, nanotechnology, optical devices and textiles [1–18]. In particular, the *ortho*-hydroxy class of Schiff bases has been attractive for physicists and chemists for many years because of its interesting photochromic and thermochromic features in the solid state. These photochromic and thermochromic features are caused by an intramolecular proton transfer from the hydroxyl O atom to the imine N atom with a change in the π-electronic system. The change in the π-electronic system accompanies the proton transfer and the planarity of molecule is affected by the transfer [19]. As the names suggest, transfer occurs under the influence of light in photochromic compounds and under the influence of temperature in thermochromic compounds. These interesting properties were discovered by Senier and Shepherd in 1909 and are still being studied today [20, 21]. *ortho*-hydroxy Schiff base compounds adopt OH (enol-imine/benzenoid) [22, 23] or NH (keto-amine/quinoid) [24, 25] tautomeric forms in the solid state with reference to the location of the transferred proton. X-ray diffraction distinguishes these two tautomeric forms easily. The NH form can also be zwitterionic, with the scarcely observed zwitterionic form differing from the NH form on the basis of the N^+-H bond distance and aromaticities of the rings [26–28]. Figure 1 shows the tautomeric forms and observed strong intramolecular hydrogen bonds depending on the forms.

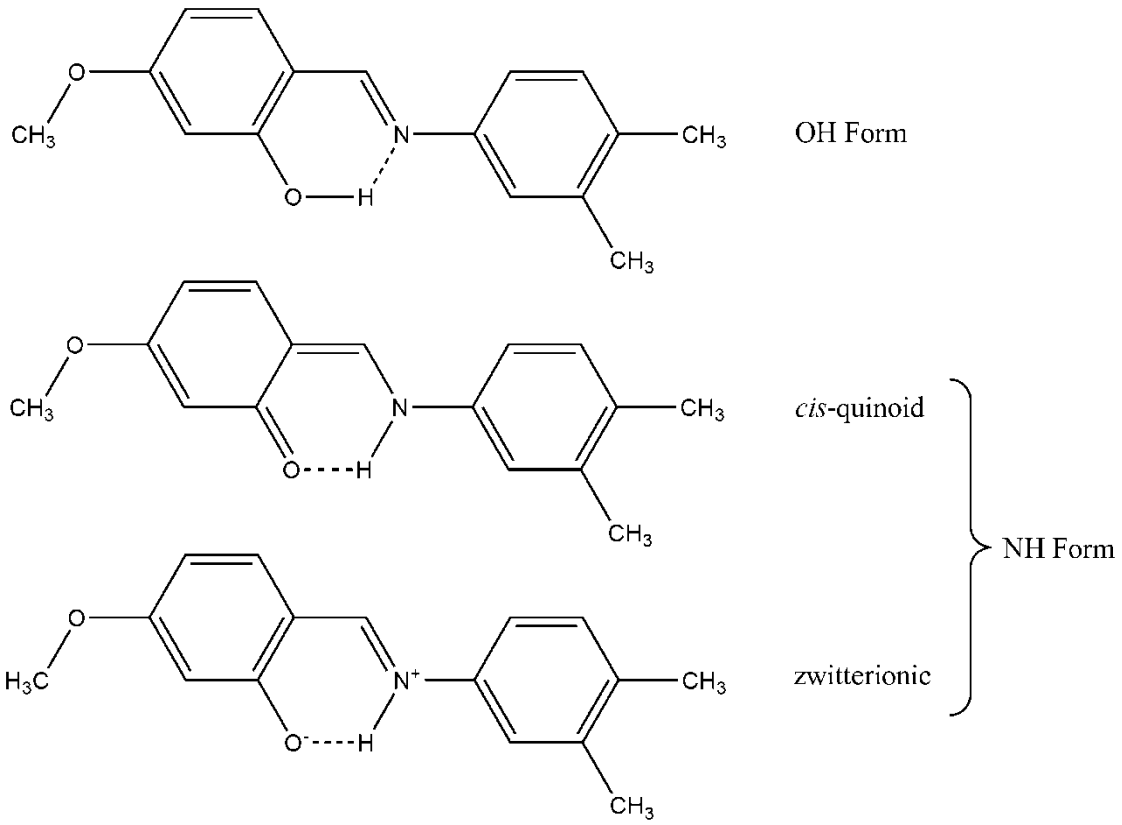

Fig. 1. Possible tautomeric forms of the title compound

In this study, we present the synthesis and crystallographic, spectroscopic and quantum chemical computational studies of an *ortho*-hydroxy Schiff base compound, (*E*)-5-methoxy-2-[(3,4-dimethylphenylimino)methyl]phenol.

2. EXPERIMENTAL AND COMPUTATIONAL PROCEDURES

2.1. *Synthesis of title compound*

The title compound was prepared by refluxing a mixture of a solution containing 2-hydroxy-4-methoxybenzaldehyde (0.5 g, 3.3 mmol) in 20 ml of ethanol and a solution containing 3,4-dimethylaniline (0.4 g, 3.3 mmol) in 20 ml of ethanol. The reaction mixture was stirred for 1 h under reflux. The crystals suitable for X-ray analysis were obtained from ethanol by slow evaporation (yield 85%, m.p 359–360 K).

2.2. *Instrumentation*

The melting point was determined by an electro-thermal melting point apparatus. The FT-IR spectrum of the title compound was recorded on a Bruker 2000 spectrometer in a KBr disk. Absorption spectra were recorded on a Unicam UV-Vis spectrometer using a 1 cm path length of the quartz cell. The ^{1}H-NMR spectrum was recorded on Bruker Ultrashield 300 MHz spectrometer. All diffraction measurements were performed at room temperature (296 K) using graphite monochromated MoKα radiation (λ = 0.71073 Å) with a Stoe IPDS 2 diffractometer.

2.3. *Crystal structure determination*

A suitable sample of size 0.68 × 0.43 × 0.28 mm^3 was chosen for the single crystal X-ray study. Reflections were collected in the rotation mode (ω scanning mode) and cell parameters were determined using X-AREA software [29]. The absorption correction (μ = 0.08 mm^{-1}) was achieved by the integration method via X-RED32 software [29]. The structure was solved by direct methods using SHELXS-97 [30]. The refinement was carried out by a full-matrix least-squares method using SHELXL-97 on the positional and anisotropic temperature parameters of the non-hydrogen atoms, or equivalently, corresponding to 176 crystallographic parameters [30]. All non-hydrogen atom parameters were refined anisotropically and H atoms, except for H1, were positioned geometrically and refined using a riding model. The C-H bond distances were fixed to 0.93 Å for CH and 0.96 Å for CH_3 groups. The U_{iso} values of H atoms were also fixed to 1.2 times the U_{eq} value of the parent atoms for CH and 1.5 times the U_{eq} value of the parent atoms for CH_3 groups. Under the condition of a $I > 2\sigma(I)$ threshold, the structure was refined to R_{int} = 0.058 with 2071 observed reflections. Other data collection conditions and parameters of the refinement process are listed in Table 1.

T a b l e 1

Crystal data and refinement parameters of the title compound

Formula	$C_{16}H_{17}NO_2$
Formula weight	255.31
Crystal color	Yellow
Crystal system	Monoclinic
Space group	$P\ 2_1/c$
Z	4
a, b, c	13.6589 (8), 6.0320 (3), 20.1848 (11) Å
α, β, γ	90, 124.606(4), 90°
V	1368.79 (13) Å^3
Radiation type	Mo Kα
μ	0.08 mm^{-1}
T_{max}, T_{min}	0.958, 0.981
Measured reflections	16076
Independent reflections	2832
Reflections with $I > 2\sigma(I)$	2071
Number of parameters	176
θ_{max}, θ_{min}	27.56°, 1.50°
Scan range	–17 < h < 17, –7 < k < 7, –26 < l < 26
$R[F^2 > 2\sigma(F^2)]$	0.0464
$wR(F^2)$	0.1225
S	1.051
$\Delta\rho_{max}$, $\Delta\rho_{min}$	0.17, –0.14 e Å^{-3}

2.4. *Supplementary data*

CCDC 942104 contains the supplementary crystallographic data for this study. These data can be obtained free of charge via www.ccdc.cam.ac.uk/data_request/cif by emailing data_request@ccdc.cam.ac.uk, or by contacting The Cambridge Crystallographic Data Centre, 12, Union Road, Cambridge CB2 1EZ, UK; fax: +44 1223 336033.

2.5. *Computational details*

The analytical gradient methods of DFT with Becke's three parameter (B3) exchange functional together with the Lee-Yang-Parr (LYP) non-local correlation functional, symbolized B3LYP [31, 32] were performed to reach the energy minima in the optimization processes of two tautomers by means of the 6-311+G(d,p) basis set implemented in the Gaussian 03W software package [33].

The crystallographically obtained coordinates were used to start the geometry optimization calculations in the gas phase and no imaginary frequency modes were obtained at the optimized geometries for the tautomers, so there are true minima on the potential energy surfaces were found for both. We also performed the optimizations in benzene (ε = 2.3), ethanol (ε = 24.5) and DMSO (ε = 46.7) using the polarizable continuum model (PCM) [34] to investigate the energetic behaviors and changes in the geometric parameters of the molecule in various environments. The PCM model can give good approximations regarding the solvent effects on the molecule if there is no specific interaction, such as hydrogen bond formation between the solute and solvent [35, 36].

In the potential energy surface (PES) scan process, the O1-H1 bond distance was taken as a redundant coordinate and varied from 0.997 to 1.697 Å with 16 steps of 0.05 Å. All the remaining internal coordinates were fully optimized. On this basis, we described the potential energy barrier belonging to the intramolecular proton transfer and observed the effects of transfer on the molecular geometry with the change in the π-electronic system.

The vibrational frequencies were calculated at the same level of theory and the obtained frequencies were scaled by 0.9688 depending on the method and basis set used [37]. The absorption spectra of the tautomers were calculated using time-dependent density functional theory (TD-DFT) started from the solution phase optimized geometries. The linear polarizability and the total static first hyperpolarizability were obtained by the molecular polarizabilities in order to show the non-linear optical (NLO) activity of the molecule. The standard thermodynamic functions and their components were computed at constant pressure (by changing the temperature) and temperature (by changing the pressure) in the gas phase.

3. RESULTS AND DISCUSSION

3.1. *Crystal structure*

Figure 2 shows an ORTEP-3 [38] plot with an atom numbering scheme for the title compound. Hydrogens are drawn as small spheres of arbitrary radii and the other atoms are seen as displacement ellipsoids at a 30% probability level.

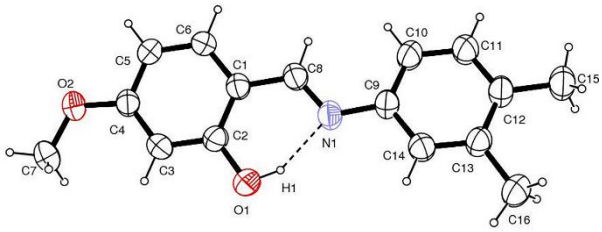

Fig. 2. Atom numbering scheme of the title compound. The dotted line indicates the intramolecular hydrogen bond.

As seen in Figure 2, the compound adopts an E configuration about the C=N double bond and has two six-membered rings, C1/C6 and C9/C14. The dihedral angle between the rings is 6.87°, which makes the molecular geometry almost planar. The literature proposes that the molecules showing thermochromism are planar and the photochromic molecules are non-planar [15, 39]. According to the planarity of the molecule, the proton transfer occurs under the influence of temperature in the title compound.

Selected geometrical parameters are listed in Table 2. The lengths of the N1=C8 double, C1=C8 single and C2-O1 single bonds indicate that the compound adopts an OH tautomeric form rather than the NH form in the solid state. The good agreement can be seen between these bond lengths and counterparts in similar OH form compounds in the literature [40, 41]. The harmonic oscillator model of aromaticity, the HOMA index, is also a sign of the aromaticity of a ring, which is why we calculated the HOMA indices for both rings using the following equation [42, 43]:

$$HOMA = 1 - \left[\frac{1}{n} \sum_{i=1}^{n} \alpha_i (R_i - R_{opt})^2 \right] \qquad (1)$$

where *n* is the number of bonds in the molecular fragments interested (in our case n is equal to 6 for the six-membered rings), the α_i normalization constant is equal to 257.7 and R_{opt} is equal to 1.388 Å for C-C bonds. For the purely aromatic systems, the HOMA index is equal to 1 and for the non-aromatic ones are equal to 0. As expected, the calculated indices of C1/C6 and C9/C14 rings are 0.950 and 0.995, respectively. The title compound displays a strong intramolecular interaction, including the O1 and N1 atoms. This type of intramolecular hydrogen bonds is a common feature of *o*-hydroxysalicylidene systems [44, 45]. The O-H, H…N, O…N and O-H…N values of the bond are 0.87 (3) Å, 1.82 (2) Å, 2.62 (2) Å and 152.00 (3)°, respectively. It can be seen from Fig. 2 that this strong hydrogen bond constitutes a S(6) ring. In the three-dimensional network, the crystal structure is stabilized by weak Van der Waals interactions.

T a b l e 2

Selected geometric parameters for (E)-5-methoxy-2-[(3,4-dimethylphenylimino)methyl]phenol

Parameters	X-ray	DFT B3LYP/6-311+G(d,p)				
		OH				NH
		Gas	Benzene	EtOH	DMSO	Gas
Bond lengths (Å)						
N1 C8	1.283 (2)	1.291	1.291	1.292	1.293	1.332
C2 O1	1.343 (2)	1.340	1.343	1.347	1.347	1.261
C1 C8	1.442 (2)	1.443	1.444	1.445	1.445	1.391
C1 C2	1.408 (2)	1.419	1.419	1.418	1.418	1.470
C1 C6	1.403 (2)	1.410	1.410	1.410	1.410	1.429
C5 C6	1.367 (2)	1.377	1.377	1.378	1.378	1.360
C4 C5	1.394 (2)	1.409	1.409	1.409	1.409	1.433
C3 C4	1.382 (2)	1.392	1.393	1.394	1.394	1.374
C2 C3	1.394 (2)	1.399	1.399	1.398	1.398	1.437
C4 O2	1.360 (2)	1.357	1.357	1.358	1.358	1.356
C7 O2	1.417 (2)	1.424	1.427	1.431	1.431	1.424
O1 H1	0.870 (2)	0.997	0.999	1.002	1.003	–
N1 H1	–	–	–	–	–	1.040
Bond angles (°)						
C1 C2 O1	121.2 (2)	121.5	121.3	121.0	121.0	121.4
C3 C2 O1	118.4 (2)	118.0	118.1	118.2	118.2	121.8
C1 C8 N1	122.4 (2)	122.4	122.2	121.9	121.8	123.0
C8 N1 C9	121.1 (2)	121.3	121.3	121.4	121.6	127.9
C5 C4 O2	114.5 (2)	115.3	115.4	115.4	115.4	113.6
C3 C4 O2	124.5 (2)	123.9	123.9	123.8	123.8	124.6
C2-O1-H1	105.9 (2)	107.2	107.0	106.7	106.7	–
Torsion angles (°)						
C6 C1 C8 N1	-175.7 (2)	179.4	179.5	179.6	179.4	179.9
C9 N1 C8 C1	179.4 (2)	176.9	177.0	177.1	177.1	178.6
C14 C9 N1 C8	170.1 (2)	146.8	147.1	149.0	150.8	169.3

3.2. *Optimized geometries of tautomers and intramolecular proton transfer process*

Table 2 also shows selected B3LYP/6-311+G(d,p) calculated geometrical parameters for both the OH and NH tautomers, besides the experimental ones. There are no significant differences between the experimental and calculated geometrical parameters of the OH form, except for the torsion angles. The planarity of the molecular geometry for the title compound is related with the torsion angles listed in last three rows of Table 2. The dihedral angle between two six-membered rings is 36.6° for the optimized OH tautomer according to the DFT calculations. The differences observed between the geometries of the experimental and calculated counterparts are caused by underestimating the intermolecular interactions.

DFT and similar calculations cannot take the intermolecular hydrogen bonds, van der Waals or dipole-dipole-like interactions into account and consider molecules in the gas phase (*in vacuo*), but in reality, the experimental results belong to the solid state consisting of interacting molecules.

Table 3 reflects the total energies, frontier orbital energies and dipole moments of both tautomeric forms of the title compound in the gas phase and also in various solvents for the OH form. The total energies of the tautomers suggest that the OH form is more stable than the NH form by ~2.4 kcal/mol in the gas phase. It is not surprising that the OH form has two aromatic rings corresponding to a more delocalized π-electronic system and generally *o*-hydroxy salicylideneanilines are observed in the OH tautomeric form. The additional information available in the table is regarding the behavior of the OH tautomer in several solvents. The interactions between the solute and solvent molecules influence the molecular geometry, vibrational frequencies, total energy, electronic spectrum and so on [46, 47]. The total energy of the title molecule decreases with the increasing polarity of solvent. The lessening of the total energy increases the stability of the molecule. Contrary to the total energy, the energy gap between the LUMOs and HOMOs and the dipole moment increase with the increasing polarity of solvent. The charge delocalization over the molecule skeleton increases and causes the dipole moment to increase.

T a b l e 3

Calculated energies, frontier orbital energies and dipole moments in the gas phase and various solvents

	E_{total} (kcal/mol)	E_{LUMO} (eV)	E_{HOMO} (eV)	μ (D)
OH form				
Gas	–517927.0356	–1.7469	–5.7946	0.7568
Benzene	–517930.3706	–1.7834	–5.8354	1.0740
EtOH	–517935.2456	–1.8563	–5.9062	1.6666
DMSO	–517935.5350	–1.8726	–5.9062	1.7193
NH form				
Gas	–517924.6259	–2.0618	–5.5304	2.6970

In order to investigate its effects on molecular geometry, the intramolecular proton transfer was investigated in the gas phase for the title compound by performing a PES scan at the B3LYP/6-311+G(d,p) level. Such an intramolecular proton transfer turns the OH tautomer into the NH tautomer, leading to important changes in the character of the molecule. The process was started from the gas phase optimized OH geometry by assigning the O1-H1 bond as a redundant internal coordinate. The relative energy versus the redundant coordinate O1-H1 bond distance in the PES scan process can be seen in Figure 3. The relative energy values are calculated with respect to the energy of the stable OH tautomer.

In Figure 3, there are two minima representing the OH and NH stable forms of the title molecule. The stable NH form is represented by a local minimum with a relative energy of 2.4 kcal/mol and the stable OH form corresponds to the global minimum. As can be seen from the potential energy curve, 4.9 kcal/mol of potential energy is needed to transform the molecule from the OH form to the NH form.

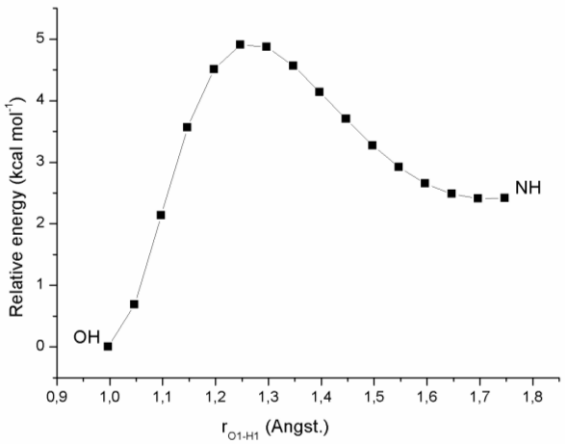

Fig. 3. Relative energy versus the redundant coordinate in the PES scan process

The effects of the intramolecular proton transfer on the molecular geometry can be clearly seen by examining the changes in the indicative bond lengths and HOMA index of the C1/C6 ring for every step in the scan process. Fig. 4 represents the changes occurring in the lengths of the C2-O1 single, C1-C8 single and C8=N1 double bonds

during the transfer process. Bond lengths of C2-O1 (1.339 Å), C1-C8 (1.443 Å) and C8=N1 (1.291 Å) belonging to the stable OH tautomer were found as 1.259, 1.390 and 1.333 Å after the fifteen step of the scan where the stable NH tautomer was observed.

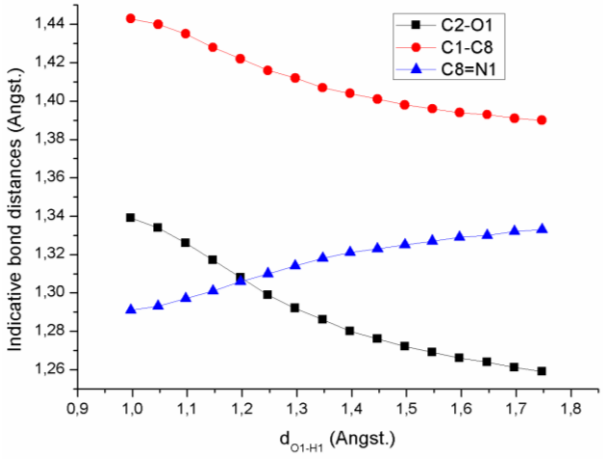

Fig. 4. Selected bond distances versus the redundant coordinate in the PES scan process

The figure clearly indicates that the intramolecular proton transfer affects the double and single characters of these bonds. The HOMA indices of the C1/C6 and C9/C14 rings were calculated at every step of the scan process. Fig. 5 shows the changes of HOMA indices in terms of the scan coordinate. The aromaticity level of the C1/C6 ring decreases while the aromaticity level of the C9/C14 ring remains stable with the scan coordinate going from 0.997 Å to 1.747 Å, as expected.

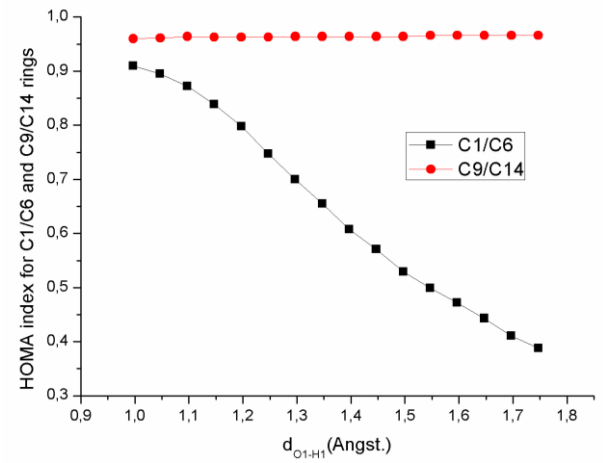

Fig. 5. HOMA indices of the rings of the molecule versus the redundant coordinate in the PES scan process.

3.3. *Electronic absorption spectra*

The UV-Vis electronic spectra of the title compound in benzene, EtOH and DMSO were measured within a 200–500 nm range at room temperature. The characteristic UV-Vis absorption bands of the molecule can be seen in Figure 6.

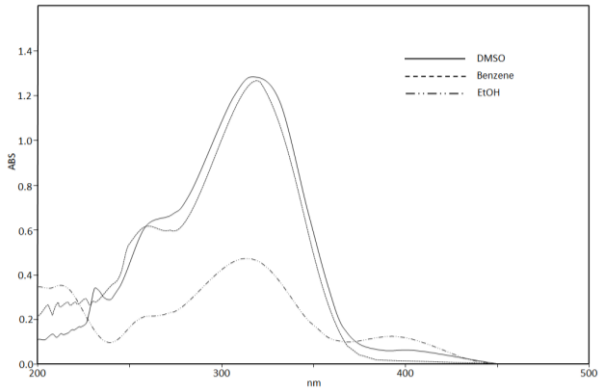

Fig. 6. Experimental UV-Vis spectra of the title compound

In the UV-Vis spectra of *ortho*-hydroxy Schiff base compounds, the presence of an absorption band at < 400 nm indicates the OH tautomeric form. Alternatively, compounds that adopt the NH tautomeric form show a new absorption band at > 400 nm [48, 49]. According to the experimental absorption spectra, the molecule exhibits absorption bands at 318 and 258 nm in benzene, at 212, 258, 318 and 392 nm in EtOH and at 232, 260, 318 and 400 nm in DMSO. Experimental spectra of the title compound show no absorption peak above 400 nm for these three solutions. The absence of the peaks above 400 nm clearly indicates that the compound adopts the OH tautomeric form, even in solution. The theoretical electronic excitation energies, oscillator strengths and nature of the first ten spin-allowed singlet-singlet excitations were calculated by the TD-DFT method for the same solvents. The major contributions of the transitions were designated with the aid of the SWizard program [50]. The experimental and calculated results of the UV-Vis spectral data are listed in Table 4.

The results obtained by the TD-DFT calculations show the absorption bands at near 370 and 280 nm. In view of the calculated absorption spectra of the OH form, the maximum absorption wavelength corresponds to the electronic transition from the HOMO to the LUMO with an 86% contribution. The other wavelengths with major contributions can be seen in Table 4.

T a b l e 4

Experimental and calculated electronic transitions of the title compound in benzene, EtOH and DMSO

	Experimental	DFT/B3LYP/6-311+G(d,p)	
	λ (nm) [A]	λ (nm) [f]	Major contributions
Benzene	318 [1.270]	348 [0.899]	H → L (86%)
	258 [0.625]	301 [0.020]	H-1 → L (84%)
		283 [0.003]	H-2 → L (49%)
			H-3 → L (31%)
			H → L+1 (14%)
		278 [0.163]	H-3 → L (43%)
			H-2 → L (28%)
			H → L+2 (10%)
		253 [0.031]	H → L+1 (54%)
			H → L+2 (13%)
			H-4 → L (12%)
		250 [0.207]	H → L+2 (43%)
			H → L+1 (19%)
			H-4 → L (15%)
EtOH	392 [0.124]	344 [0.871]	H → L (85%)
	314 [0.468]	299 [0.013]	H-1 → L (82%)
	258 [0.212]	283 [0.003]	H-2 → L (66%)
			H-3 → L (15%)
	212 [0.350]	277 [0.168]	H-3 → L (56%)
			H-2 → L (13%)
		252 [0.018]	H → L+2 (49%)
			H-4 → L (18%)
			H → L+1 (13%)
		249 [0.203]	H → L+1 (58%)
			H-4 → L (14%)
			H-2 → L (7%)
DMSO	400 [0.090]	346 [0.898]	H → L (86%)
	318 [1.277]	299 [0.014]	H-1 → L (82%)
	260 [0.635]	284 [0.003]	H-2 → L (67%)
			H-3 → L (15%)
			H → L+2 (8%)
	232 [0.348]	277 [0.169]	H-3 → L (57%)
			H-2 → L (13%)
			H → L+1 (8%)
		252 [0.019]	H → L+2 (53%)
			H-4 → L (18%)
			H → L+1 (9%)
		249 [0.216]	H → L+1 (61%)
			H-4 → L (13%)
			H-2 → L (7%)

3.4. *Vibrational frequencies*

The FT-IR spectrum of the title compound is given in Fig. 7, with the experimental and scaled computational vibrational frequencies of the compound compared in Table 5.

The O-H stretching can be attributed to the remarkable absorption band in the 2000–3000 cm^{-1} region in the experimental spectrum. The intramolecular and intermolecular hydrogen bond formations affect the O-H stretching vibration. The strong intramolecular hydrogen bond between the O1 and N1 atoms of the title molecule causes this phenomenon here and the experimental vibrational frequency of O-H stretching is shifted and widened to the 2000–3000 cm^{-1} range.

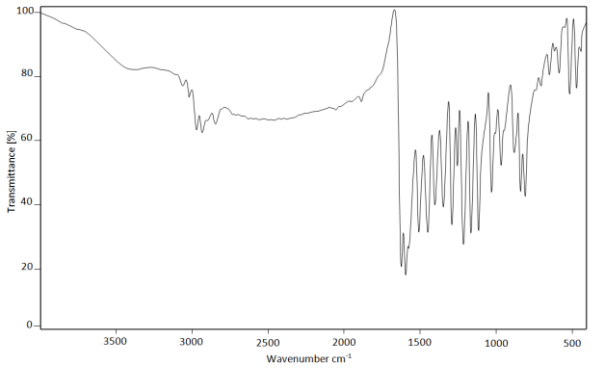

Fig. 7. Experimental FT-IR spectrum of the title compound

The O-H in-plane and out-of-plane bending vibrations are located at 1343 and 794 cm^{-1}, respectively. The band located at 1620 cm^{-1} can be attributed to C=N stretching. The spectrum also shows the presence of C-O stretching at 1213 cm^{-1}.While the absorption bands located at 2833–2906 cm^{-1} region belong to symmetric CH_3 stretching, the bands of asymmetric CH_3 stretching can be seen in the 2931–2967 cm^{-1} region. Table 5 shows the other vibrational frequencies and scaled computational vibrational frequencies of the compound. These frequency values are in good agreement with the literature [51, 52]. The theoretical results obtained from DFT calculations show good agreement with the experimental values, except for the O-H stretching.

T a b l e 5

Experimental and calculated vibrational frequencies of IR spectra (cm^{-1})

Assignments	Experimental	DFT/B3LYP/6-311+G(d,p)
Aromatic CH out of plane bending	807–835	786–795
Aromatic CH bending	1025	1018
CO stretching	1213	1219
OH bending	1343	1388
Symmetric CH_3 bending	1397	1366
Asymmetric CH_3 bending	1448	1449
Aromatic CC stretching	1590	1547
CN stretching	1620	1610
OH stretching	2455	3038
Symmetric CH_3 stretching	2833–2906	2918
Asymmetric CH_3 stretching	2931–2967	2962
Aromatic CH stretching	3012	3056

3.5. *^{1}H NMR spectra*

The ^{1}H-NMR spectrum of the title compound was recorded in DMSO-d_6 and can be seen in Fig. 8. The resonance of the hydroxyl proton is at 13.86 ppm. As expected, this is typical for protons involved in intramolecular hydrogen bonding. The resonance of the imino proton is at 8.82 ppm. The absorption peaks of aromatic ring protons are between 6 and 8 ppm. The H3 proton is coupled to the H5 proton and shows doublet peaks at 6.47 ppm ($J_{3,5}$ = 2.32 Hz). The H5 proton coupled to H6 shows a doublet and gives another doublet by coupling to H3 at 6.53 ppm ($J_{5,6}$ = 8.6 Hz, $J_{5,3}$ = 2.32 Hz). The H6 proton is coupled to the H5 proton and shows a doublet at 7.5 ppm ($J_{6,5}$ = 8.6 Hz). The H8 proton is coupled to the H12 proton and shows doublet peaks at 7.17 ppm ($J_{8,12}$ = 2.76 Hz). The H12 proton coupled to H11 shows a doublet and gives another doublet by coupling to H8 at 7.11 ppm ($J_{12,11}$ = 8 Hz, $J_{12,8}$ = 2.76 Hz). The H11 proton is coupled to the H12 proton and shows a doublet at 7.18 ppm. The resonances of the H15, H16 and H17 protons are at 2.22, 2.25 and 3.80 ppm, respectively. The absorption of ring protons is in the range of 6–8 ppm, which corresponds to an aromatic character. These results are in a good agreement with the literature and also show that the title compound adopts an OH form in solution [40, 51].

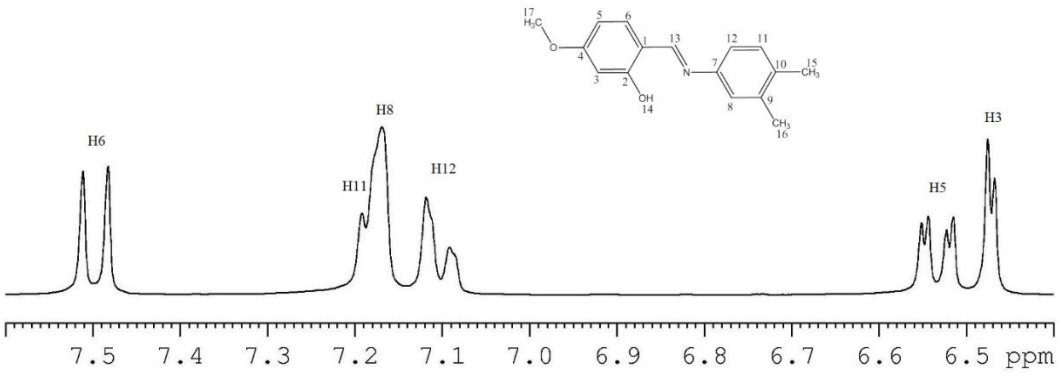

Fig. 8. Experimental ^{1}H NMR spectrum of the title compound

3.6. *Second-order NLO properties*

The NLO properties of a molecule, which can be predicted by quantum chemical calculations, play an important role for the design of new materials in communication, signal processing and optical interconnection technologies [53]. In particular, organic molecules are studied frequently because of their larger NLO susceptibilities, with π-electron cloud movement from donor to acceptor, fast NLO response times, high laser damage thresholds and low dielectric constants. In addition to these advantages, the organic molecules also have disadvantages, including generally low thermal stability, facile relaxation to random orientations and in the UV-Vis region, the low energy transitions result in a trade-off between their nonlinear efficiency and optical transparency [54–56]. The usage of organic molecules as ligands can overcome the disadvantages. Their usage as ligands allows the Schiff base compounds to be investigated for this field.

The average linear polarizability $\bar{\alpha}$ and the first hyperpolarizability β can be calculated by using the Eqs. (2) and (3), respectively [53]:

$$\bar{\alpha} = \frac{1}{3}\left(\alpha_{xx} + \alpha_{yy} + \alpha_{zz}\right) \quad (2)$$

$$\beta = \left[\left(\beta_{xxx} + \beta_{xyy} + \beta_{xzz}\right)^2 + \left(\beta_{yyy} + \beta_{xxy} + \beta_{yzz}\right)^2 + \left(\beta_{zzz} + \beta_{xxz} + \beta_{yyz}\right)^2\right]^{1/2} \quad (3)$$

In order to investigate the NLO properties of the title compound, the components of dipole moment, polarizability and the first hyperpolarizability have been calculated using polar = ENONLY input to Gaussian03 at the level of B3LYP/6-311+G(d,p) in the gas phase. The components and calculated values of the average linear polarizability $\bar{\alpha}$ and the first hyperpolarizability β are listed in Table 6.

The calculated values of components show a difference depending on the size of the basis sets used. However, it is difficult to decide which basis set generates reliable values because there are no reported experimental values for the title compound in the literature. For this reason, we used the basis set 6-311+G(d,p) in all this work. The calculated β components have been converted into electrostatic units esu (1 au = 8.6393×10^{-33} esu). The values of $\bar{\alpha}$ and β obtained by Sun *et al.* with the B3LYP/6-31G(d) method for urea are 3.831 Å^3 and 0.372×10^{-30} esu, respectively, and generally used for the comparison [57]. In present work, the value of $\bar{\alpha}$ is 126.634 Å^3 and the value of β is 107.516×10^{-30} esu for the title molecule. The movement of the π-electron cloud must be responsible for the increasing conjugation, and hence an increase in the NLO properties of the molecule. According to the high value of the first hyperpolarizability, the title compound could be an excellent applicant in the development of NLO materials.

Table 6

Calculated polarizability (Å^3) and the first hyperpolarizability ($\times 10^{-30}$ esu) components for (E)-5-methoxy-2-[(3,4-dimethylphenylimino)methyl]phenol

α_{xx}	60.4372
α_{xy}	–0.4112
α_{yy}	28.9580
α_{xz}	0.2703
α_{yz}	–0.0925
α_{zz}	18.3818
β_{xxx}	–11.0507
β_{xxy}	–3.2233
β_{xyy}	1.1893
β_{yyy}	–0.8852
β_{xxz}	1.1907
β_{xyz}	–0.4443
β_{yyz}	0.2199
β_{xzz}	0.1499
β_{yzz}	–0.2689
β_{zzz}	0.0458

3.7. *Thermodynamic properties*

The standard thermodynamic functions, such as enthalpy (H^0_m), entropy (S^0_m), heat capacity ($C^0_{p,m}$), thermal energy (E) and their components, were computed at constant pressure (by changing the temperature) and temperature (by changing the pressure) in the gas phase with the B3LYP/6-311G+(d,p) level of theory. The changes of all thermodynamic functions at various temperatures and pressures in the range of 100.00–500.00 K and 1.00–5.00 atm are given in Table 7. The total energy of a molecular system is the sum of the translation, electronic, rotational and vibrational energies. To obtain the total energy of the molecule, the contribution of these energy values to the thermal energy, heat capacity and entropy values were obtained. In addition, the component of rotational temperatures and constants were calculated (see Table 7). The values of thermal energy components are the same at all pressures but change with changing temperature. These values are 0.000 for

T a b l e 7

Calculated thermodynamic components for (E)-5-methoxy-2-[(3,4-dimethylphenylimino)methyl]phenol

		Thermal energy, E (cal/mol K)	$C^{0}_{p,m}$ **(cal/mol K)**	S^{0}_{m} **(cal/mol K)**	***P(atm)=1***		H^{0}_{m} **(kcal/mol)**
electronic	T(K) = 100	0.000	0.000	0.000		*0.000*	1.830
translational		0.889	2.981	37.083		*42.510*	
rotational		0.889	2.981	30.732		*33.988*	
vibrational		193.842	21.602	18.265		*59.988*	
total		**195.620**	**27.564**	**86.080**		***136.487***	
	150	0.000	0.000	0.000	***1.5***	*0.000*	3.566
		0.447	2.981	39.097		*41.704*	
		0.447	2.981	31.941		*33.988*	
		186.900	31.834	28.979		*59.988*	
		187.794	**37.795**	**100.016**		***135.681***	
	200	0.000	0.000	0.000	***2***	*0.000*	5.805
		0.596	2.981	40.526		*41.132*	
		0.596	2.981	32.798		*33.988*	
		188.742	41.872	39.508		*59.988*	
		189.934	**47.834**	**112.833**		***135.109***	
	250	0.000	0.000	0.000	***2.5***	*0.000*	8.552
		0.745	2.981	41.635		*40.689*	
		0.745	2.981	33.463		*33.988*	
		191.091	52.132	49.949		*59.988*	
		192.581	**58.093**	**125.048**		***134.666***	
B3LYP	***298.150***	*0.000*	*0.000*	*0.000*			***11.686***
		0.889	*2.981*	*42.510*			
		0.889	*2.981*	*33.988*			
		193.842	*62.154*	*59.988*			
		195.620	***68.116***	***136.486***			
	300	0.000	0.000	0.000	***3***	*0.000*	11.889
		0.894	2.981	42.541		*40.327*	
		0.894	2.981	34.007		*33.988*	
		193.958	62.538	60.374		*59.988*	
		195.746	**68.500**	**136.921**		***134.303***	
	350	0.000	0.000	0.000	***3.5***	*0.000*	15.598
		1.043	2.981	43.306		*40.020*	
		1.043	2.981	34.466		*33.988*	
		197.342	72.781	70.788		*59.988*	
		199.429	**78.743**	**148.560**		***133.997***	
	400	0.000	0.000	0.000	***4***	*0.000*	19.881
		1.192	2.981	43.970		*39.755*	
		1.192	2.981	34.864		*33.988*	
		201.228	82.546	81.150		*59.988*	
		203.612	**88.508**	**159.985**		***133.732***	
	450	0.000	0.000	0.000	***4.5***	*0.000*	24.636
		1.341	2.981	44.555		*39.521*	
		1.341	2.981	35.216		*33.988*	
		205.585	91.630	91.405		*59.988*	
		208.268	**97.592**	**171.175**		***133.498***	
	500	0.000	0.000	0.000	***5***	*0.000*	29.826
		1.490	2.981	45.078		*39.312*	
		1.490	2.981	35.530		*33.988*	
		210.378	99.948	101.496		*59.988*	
		213.359	**105.910**	**182.104**		***133.288***	

electronic, 0.889 for translation and rotational, 193.842 for vibrational and 195.620 for the total energy at all pressures. Otherwise, all the components of the entropy show different values at different temperatures. The translational energy shows different values under varying pressure, but the electronic energy is equal to zero at all pressures. The other two components have the same value at all pressures. It is clear that the thermal energies come from the vibration energy of the greatest contribution. The results show that the standard thermodynamic functions increase with

increasing temperature, due to the intensities of increasing molecular vibration. It has been shown that the entropy increases, otherwise the enthalpy and heat capacity remain stable, when the pressure is increased at 298.15 K. Finally, the calculated zero-point vibrational energy, the components of rotational temperatures and constants for the title compound are 184.52595 Kcal/mol; 0.06715, 0.0610, 0.0569 K and 1.39911, 0.12700, 0.11861 GHz at all the temperatures and pressures, respectively.

4. CONCLUSIONS

In this study, we synthesized a Schiff base compound, (*E*)-5-methoxy-2-[(3,4-dimethylphenylimino)methyl]phenol, and characterized it by spectroscopic, structural and theoretical methods. X-ray, FT-IR, UV-Vis and NMR methods confirm the OH form of the title compound for the gas phase and in solution. The optimized molecular geometry obtained from the DFT B3LYP/6-311+G(d,p) calculations is very close to the molecular geometry in the solid crystal structure. In the gas phase, the PES scan process shows that the potential barrier to exceed the transition from the OH tautomeric form to the NH tautomeric form is 4.9 kcal/mol. This intramolecular proton transfer affects the molecular geometry effectively by changing the aromaticity of the C1/C6 ring and indicative bond lengths. The high value of the first hyperpolarizability shows that the title compound can be used as a new material in non-linear optical studies. We hope this study will help researchers to design and synthesize new materials.

REFERENCES

[1] W. M. F. Fabian, L. Antonov, D. Nedeltcheva, F. S. Kanounah, P. J. Taylor, Tautomerism in hydroxynaphthaldehyde anils and azo analogues: a combined experimental and computational study, *J. Phys. Chem.*, **A108** (2004) 7603–7612. DOI: 10.1021/jp048035z

[2] T. M. Krygowski, J. E. Zachara-Horegland, M. Palusiak, S. Pelloni, P. Lazzaretti, Relation between pi-electron localization/delocalization and H-bond strength in derivatives of o-hydroxy-Schiff bases, *J. Org. Chem.*, **73** (2008) 2138–2145. DOI: 10.1021/jo7023174

[3] V. Bertolasi, P. Gilli, G. Gilli, Crystal Chemistry and Prototropic Tautomerism in 2-(1-Iminoalkyl)- phenols (or naphthols) and 2-Diazenyl-phenols (or naphthols), *Curr. Org. Chem.*, **13** (2009) 250–268. DOI: 10.2174/138527209787314841

[4] B. Kukawska-Tarnawska, A. Les, T. Dziembowska, Z. J. Rozwadowski, Tautomeric forms of N-(5-nitrosalicylidene)-2-butylamine: Experimental and theoretical DFT study, *J. Mol. Struct*., **928** (2009) 25–31. DOI: 10.1016/j.molstruc.2009.03.007

[5] H. Ünver, K. Polat, M. Uçar, D. M. Zengin, Synthesis and keto-enol tautomerism in N-(2-hydroxy-1-naphthylidene)anils, *Spect. Lett.*, **36** (4) (2003) 287–301. DOI: 10.1081/SL-120024579

[6] D. Maciejewska, D. Pawlak, V. Koleva, Hydrogen bonding and tautomerism of benzylideneanilines in the solid state, *J. Phys. Org. Chem.*, **12** (1999) 875–880.

[7] H. Karabıyık, H. Petek, N. Ocak-İskeleli, Ç. Albayrak, Structural and aromatic aspects for tautomerism of (Z)-6-((4-bromophenylamino)methylene)-2,3-dihydroxycyclohexa-2,4-dienone, *Struct. Chem.* **20** (2009) 1055–1065. DOI: 10.1007/s11224-009-9509-x

[8] H. Petek, Ç. Albayrak, M. Odabaşoğlu, İ. Şenel, O. Büyükgüngör, The proton transfer process observed in the structure analysis and DFT calculations of (E)-2-ethoxy-6-[(2-methoxyphenylimino)methyl]phenol, *Struct. Chem*., **21** (2010) 681–690. DOI: 10.1007/s11224-010-9598-6

[9] A. D. Garnovski, A. L. Nivorozhki, V. I. Minkin, Ligand environment and the structure of Schiff base adducts and tetracoordinated metal-chelates, Coord. *Chem. Rev*., **126** (1993) 1–69. DOI: 10.1016/0010-8545(93)85032-Y

[10] M. Calligaris, L. Randaccio, In: G. Wilkinson (Ed.), *Compherensive Coordination Chemistry*, Vol **2**, Permagon Press, London, pp. 715–738, 1987.

[11] R. H. Lozier, R. A. Bogomolni, W. Stoeckenius, Bacteriorhodopsin: A light-driven proton pump in Halobacterium halobium, *Biophys. J*., **15,** (1975) 955–962. DOI: 10.1016/S0006-3495(75)85875-9

[12] A. Das, M. D. Trousdale, S. Ren, E. J. Lien, Inhibition of herpes simplex virus type 1 and adenovirus type 5 by heterocyclic Schiff bases of aminohydroxyguanidine tosylate, *Antiviral Res*., **44** (1999) 201–208. DOI: 10.1016/S0166-3542(99)00070-4

[13] S. Ren, R. Wang, K. Komatsu, P. Bonaz-Krause, Y. Zyrianow, C. E. McKenna, C. Osipke, Z. A. Tokes, E. J. Lien, Synthesis, biological evaluation, and quantitative structure-activity relationship analysis of new Schiff bases of hydroxysemicarbazide as potential antitumor agents, *J. Med. Chem.*, **45** (2002) 410–419. DOI: 10.1021/jm010252q

[14] S. Ren, Z. A. Tokes, C. Osipke, B. Zhou, Y. Yen, E. J. Lien, Inhibition of tumor cell growth by Schiff bases of hydroxysemicarbazide, *Anticancer Res*., **21** (2001) 3445–3451.

[15] E. Hadjoudis, M. Vitterakis, I. Moustakali-Mavridis, Photochromism and thermochromism of Schiff-bases in the solid-state and in rigid glasses, *Tetrahedron* **43** (1987) 1345–1360. DOI: 10.1016/S0040-4020(01)90255-8

[16] E. Hadjoudis, Photochromic and thermochromic anils, *Mol. Eng.* **5** (4) (1995) 301–337. DOI: 10.1007/BF01004014

[17] A. P. Alivisatos, P. F. Barbara, A. W. Castleman, J. Chang, D. A. Dixon, M. L. Klein, G. L. McLendon, J. S. Miller, M. A. Ratner, P. J. Rossky, S. I. Stupp, M. E. Thomson, From molecules to materials: Current trends and future directions, *Adv. Materials.*, **10** (16) (1998) 1297–1336.

[18] L. Dalton, Polymers for photonics applications I, *Adv. Polym. Sci*., **158** (2002) 1–75. DOI: 10.1007/3-540-44608-7

[19] A. Koll, J. Janski, A. Karpfen, P. Wolschann, Bifunctional influence of 3-chloro substitution on structural and energetic characteristics of N-methyl-salicylidene imines, *J. Mol. Struct*., **976** (2010) 19–29. DOI: 10.1016/j.molstruc.2009.12.028

[20] A. Senier, F. G. Shepheard, Studies in phototropy and thermotropy. Part 1. Arylidene and naphthylideneamines, *J. Chem. Soc*., **95** (1909) 1943–1955. DOI: 10.1039/CT9099501943

[21] A. Filarowski, A. Kochel, K. Cieslik, A. Koll, Steric and aromatic impact on intramolecular hydrogen bonds in *o*-hydroxyaryl ketones and ketimines, *J. Phys. Org. Chem.*, **18** (2005) 986–993. DOI: 10.1002/poc.942

[22] G. Pavlovic, J. M. Sosa, A 3-[(2-Oxo-1-naphthylidene) methylamino]benzoic acid, *Acta Cryst.* C56 (2000) 1117–1119. DOI: 10.1107/S0108270100007290

[23] R. Casasnovas, A. Salva, J. Frau, J. Donoso, F. Munoz, Theoretical study on the distribution of atomic charges in the Schiff bases of 3-hydroxypridine-4-aldehyde and alanine. The effect of the protonation state of the pyridine and imine nitrogen atoms, *Chem. Phys.*, **355** (2009) 149–156. DOI: 10.1016/j.chemphys.2008.12.006

[24] H. Ünver, M. Yıldız, Tautomerism in solution and solid state, spectroscopic studies and crystal structure of (Z)-1-[(4-amino-2,3,5,6-tetramethylphenylamino)methylene]-1, 8a-dihydronaphthalen-2(3H)-one, *Spect. Lett*., **43** (2010) 114–121. DOI: 10.1080/00387010903284646

[25] T. Dziembowska, M. Szafran, A. Katrusrak, Z. Raqzwadowski, Crystal structure of and solvent effect on tautomeric equilibrium in Schiff base derived from 2-hydroxy-1-napthaldehyde and methylamine studied by X-ray diffraction, DFT, NMR and IR methods, *J. Mol. Struct*., **929** (2009) 32–42. DOI: 10.1016/j.molstruc.2009.04.001

[26] H. Petek, Ç. Albayrak, N. Ocak-İskeleli, E. Ağar, İ. Şenel, Crystallographic and conformational analyses of zwitterionic form of (*E*)-2-methoxy-6-[(2-morpholinoethylimino)methyl]phenolate, *J. Chem. Cryst*., **37** (2007) 285–290. DOI: 10.1007/s10870-006-9175-4

[27] G. Wojciechowski, M. Ratajczak-Sitarz, A. Katrusiak, W. Schilf, P. Przybylski, B. Brzezinski, Crystal structure of Schiff base derivative of gossypol with 3,6,9-trioxadecylamine, *J. Mol. Struct.*, **650** (2003) 191–199. DOI: 10.1016/S0022-2860(03)00319-3

[28] H. Petek, Ç. Albayrak, E. Ağar, H. Kalkan, (Z)-6-[(2-Fluorophenyliminio)methylene]-2,3-dihydroxyphenolate, *Acta Cryst.*, **E62** (2006) o3685-o3687. DOI: 10.1107/S1600536806029606

[29] Stoe & Cie, X-AREA (Version 1.18) and X-RED32 (Version 1.04), Darmstadt, Germany, 2002.

[30] G. M. Sheldrick, A short history of SHELX, *Acta Cryst.* **A64** (2008) 112–122. DOI: 10.1107/S0108767307043930

[31] C. Lee, W. Yang, R. G. Parr, Development of the Colle-Salvetti correlation-energy formula into a functional of the electron density, *Phys. Rev*., **B37** (1988) 785–789. DOI: 10.1103/PhysRevB.37.785

[32] A. D. Becke, Density-functional thermochemistry. III. The role of exact exchange, *J. Chem. Phys*., **98** (1993) 5648–5652. DOI: 10.1063/1.464913

[33] M. J. Frisch, G. W. Trucks, H. B. Schlegel, G. E. Scuseria, M. A. Robb, J. R. Cheeseman, J. A. Montgomery, Jr., T. Vreven, K. N. Kudin, J. C. Burant, J. M. Millam, S. S. Iyengar, J. Tomasi, V. Barone, B. Mennucci, M. Cossi, G. Scalmani, N. Rega, G. A. Petersson, H. Nakatsuji, M. Hada, M. Ehara, K. Toyota, R. Fukuda, J. Hasegawa, M. Ishida, T. Nakajima, Y. Honda, O. Kitao, H. Nakai, M. Klene, X. Li, J. E. Knox, H. P. Hratchian, J. B. Cross, V. Bakken, C. Adamo, J. Jaramillo, R. Gomperts, R. E. Stratmann, O. Yazyev, A. J. Austin, R. Cammi, C. Pomelli, J. W. Ochterski, P. Y. Ayala, K. Morokuma, G. A. Voth, P. Salvador, J. J. Dannenberg, V. G. Zakrzewski, S. Dapprich, A. D. Daniels, M. C. Strain, O. Farkas, D. K. Malick, A. D. Rabuck, K. Raghavachari, J. B. Foresman, J. V. Ortiz, Q. Cui, A. G. Baboul, S. Clifford, J. Cioslowski, B. B. Stefanov, G. Liu, A. Liashenko, P. Piskorz, I. Komaromi, R. L. Martin, D. J. Fox, T. Keith, M. A. Al-Laham, C. Y. Peng, A. Nanayakkara, M. Challacombe, P. M. W. Gill, B. Johnson, W. Chen, M. W. Wong, C. Gonzalez, and J. A. Pople, Gaussian, Inc., Wallingford CT, 2004.

[34] J. Tomasi, B. Mennucci, R. Cammi, Quantum mechanical continuum solvation models, *Chem. Rev*., **105** (2005) 2999–3093. DOI: 10.1021/cr9904009

[35] D. Jacquemin, J. Preat, V. Wathelet, M. Fontaine, E. A. Perpete, Thioindigo Dyes: Highly Accurate Visible Spectra with TD-DFT, *J. Am. Chem. Soc*., **128** (2006) 2072–2083. DOI: 10.1021/ja056676h

[36] N. Santhanamoorthi, K. Senthilkumar, P. Kolandaivel, Tautomerization and solvent effects on the absorption and emission properties of the Schiff base N,N′-bis(salicylidene)-p-phenylenediamine - A TDDFT study, *Mol. Phys.*, **108** (14) (2010) 1817–1827. DOI: 10.1080/00268976.2010.490796

[37] J. P. Merrick, D. Moran, L. Radom, An evaluation of harmonic vibrational frequency scale factors, *J. Phys. Chem*., **A111** (2007) 11683–11700. DOI: 10.1021/jp073974n

[38] L. J. Farrugia, *ORTEP*-3 for Windows - a version of *ORTEP*-III with a Graphical User Interface (GUI), *J. Appl. Cryst*., 30 (1997) 565. DOI: 10.1107/S0021889897003117

[39] I. Moustakali-Mavridis, E. Hadjoudis, A. Mavridis, Structure of thermochromic Schiff bases. II. Structures of N-salicylidene-3-aminopyridine and N-(5-methoxysalicylidene)-3-aminopyridine, *Acta Cryst*., **B36** (1980) 1126–1130. DOI: 10.1107/S0567740880005432

[40] Ç. Albayrak, G. Kaştaş, M. Odabaşoğlu, R. Frank, The prototropic tautomerism and substituent effect through strong electron withdrawing group in (E)-5-(diethylamino)-2-[(3-nitrophenylimino)methyl]phenol, *Spectrochimica Acta Part A*, **114** (2013) 205–213. DOI: 10.1016/j.saa.2013.05.044

[41] D. K. Dey, S. P. Dey, A. Elmalı, Y. Elerman, Molecular structure and conformation of N-2-[3'-(methoxysalicylideneimino)benzyl]-3"-methoxysalicylideneimine, *J. Mol. Struct*., **562** (2001) 177–184. DOI: 10.1016/S0022-2860(00)00970-4

[42] J. Kruszewski, T. M. Krygowski, Definition of Aromaticity Basing on the Harmonic Oscillator Model, *Tetrahedron Lett.*, **13** (1972) 3839–3842. DOI: 10.1016/S0040-4039(01)94175-9

[43] T. M. Krygowski, M. K. Cyrański, Structural Aspects of Aromaticity, *Chem. Rev.*, **101** (2001) 1385–1419. DOI: 10.1021/cr990326u

[44] M. Yıldız, Z. Kılıç, T. Hökelek, Intramolecular hydrogen bonding and tautomerism in Schiff bases. Part 1. Structure of 1,8-di[N-2-oxyphenyl-salicylidene]-3,6-dioxaoctane, *J. Mol. Struct*., **441** (1998) 1–10. DOI: 10.1016/S0022-2860(97)00291-3

[45] A. Filarowski, A. Koll, T. Glowiak, Structure and hydrogen bonding in ortho-hydroxy ketimines, *J. Mol. Struct*., **644** (2003) 187–195. DOI: 10.1016/S0022-2860(02)00489-1

[46] M. Odabaşoğlu, Ç. Albayrak, R. Özkanca, F.Z. Aykan, P. Lonecke, Some polyhydroxy azo–azomethine derivatives of salicylaldehyde: Synthesis, characterization, spectroscopic, molecular structure and antimicrobial activity studies, *J. Mol. Struct.*, **840** (2007) 71–89. DOI: 10.1016/j.molstruc.2006.11.025

[47] R. Dobosz, A. Skotnicka, Z. Rozwadowski, T. Dziembowska, Stability of N-(ortho-hydroxynaphthylmethylene)methylamines and their tautomers, *J. Mol. Struct*., **979** (2010) 194–199. DOI: 10.1016/j.molstruc.2010.06.024

[48] K. Ogawa, J. Harada, Aggregation controlled proton tautomerization in salicylideneanilines, *J. Mol. Struct*., **647** (2003) 211–216. DOI: 10.1016/S0022-2860(02)00526-4

[49] S. I. Gorelsky, SWizard program, Revision 4.5. http://www.sg.chem.net/, University of Ottawa, Ottawa, Canada, 2010.

[50] H. Nazır, M. Yıldız, H. Yılmaz, M. N. Tahir, D. Ülkü, Intramolecular hydrogen bonding and tautomerism in Schiff bases, *J. Mol. Struct*., **524** (2000) 241–250. DOI: 10.1016/S0022-2860(00)00393-8

[51] R. M. Silverstein, F. X. Webster, D. J. Kiemle, Spectrometric Identification of Organic Compounds, 7th ed. John Wiley & Sons, New York, 2005. DOI: 10.1021/ed039p546

[52] B. Koşar, Ç. Albayrak, C. C. Ersanlı, M. Odabaşoğlu, O. Büyükgüngör, Molecular structure, spectroscopic investigations, second-order nonlinear optical properties and intramolecular proton transfer of (*E*)-5-(diethylamino)-2-[(4-propylphenylimino)methyl]phenol: A combined experimental and theoretical study, *Spectrochimica Acta Part A*, **93** (2012) 1–9. DOI: 10.1016/j.saa.2012.03.004

[53] D. Sajan, J. Hubert, V. S. Jayakumar, J. Zaleski, Structural and electronic contributions to hyperpolarizability in methyl p-hydroxy benzoate, *J. Mol. Struct*., **785** (2006) 43–53. DOI: 10.1016/j.molstruc.2005.09.041

[54] C. E. Powel, M. G. Humphrey, Nonlinear optical properties of transition metal acetylides and their derivatives, *Coord. Chem. Rev*., **248** (2004) 725–756. DOI: 10.1016/j.ccr.2004.03.009

[55] K. S. Thanthiriwatte, K. M. Nalin de Silva, Non-linear optical properties of novel fluorenyl derivatives-ab initio quantum chemical calculations, *J. Mol. Struct., Theochem* **617** (2002) 169–175. DOI: 10.1016/S0166-1280(02)00419-0

[56] L. Fang, G. C. Yang, Y. Q. Qiu, Z. M. Su, Theoretical predication of third-order optical nonlinearities of $[Al_4MAl_4]^{n-}$ (n = 0–2, M = Ti, V and Cr) clusters, *Theor. Chem. Account*., **119** (2008) 329–333. DOI: 10.1007/s00214-007-0388-1

[57] Y. X. Sun, Q. L. Hao, W. X. Wei, Z. X. Yu, L. D. Lu, X. Wang, Y. S. Wang, Experimental and density functional studies on 4-(3,4-dihydroxybenzylideneamino)antipyrine, and 4-(2,3,4-trihydroxybenzylideneamino)antipyrine, *J. Mol. Struct. Theochem.*, **904** (2009) 74–82. DOI: 10.1016/j.theochem.2009.02.036